Image Metric-based Biometric Comparators: A Supplement to Feature Vector-based Hamming Distance?

H. Hofbauer[1], C. Rathgeb[1,2], A. Uhl[1], and P. Wild[1]
[1]Multimedia Signal Processing and Security Lab (WaveLab)
Department of Computer Sciences, University of Salzburg, Austria
[2]Center for Advanced Security Research Darmstadt (CASED), Germany
Email: {hhofbaue,crathgeb,uhl,pwild}@cosy.sbg.ac.at

***Abstract*—In accordance with the ISO/IEC FDIS 19794-6 standard an iris-biometric fusion of image metric-based and Hamming distance (HD) comparison scores is presented. In order to demonstrate the applicability of a knowledge transfer from image quality assessment to iris recognition, Peak Signal to Noise Ratio (PSNR), Structural Similarity Index Measure (SSIM), Local Edge Gradients metric (LEG), Edge Similarity Score (ESS), Local Feature Based Visual Security (LFBVS), and Visual Information Fidelity (VIF) are applied to iris textures, i.e. query textures are interpreted as noisy representations of registered ones. Obtained scores are fused with traditional HD scores obtained from iris-codes generated by different feature extraction algorithms. Experimental evaluations on the CASIA-v3 iris database confirm the soundness of the proposed approach.**

I. Introduction

Iris recognition takes advantage of random variations in the iris. The details of each iris are phenotypically unique yielding recognition rates above 99% and equal error rates of less than 1% on diverse data sets. In past years the ever-increasing demand on biometric systems operating in less constrained environments entails continuous proposals of new iris feature extraction methods [1]. Still, the processing chain of traditional iris recognition (and other biometric) systems has been left almost unaltered, following Daugman's approach [2] consisting of (1) segmentation and preprocessing, (2) feature extraction, and (3) biometric comparison.

The International Organization for Standardization (ISO) specifies iris biometric data to be recorded and stored in (raw) image form (ISO/IEC FDIS 19794-6), rather than in extracted templates (e.g. iris-codes) achieving more interoperability as well as vendor neutrality [3]. Biometric databases, which store raw biometric data, enable the incorporation of future improvements (e.g. in segmentation stage) without re-enrollment of registered users. While the extraction of rather short (a few hundred bytes) binary feature vectors provides a compact storage and rapid comparison of biometric templates, information loss is inevitable. This motivates a fusion of comparators operating in image domain (e.g. image metrics) and traditional HD-based comparators requiring binary feature vectors. The contribution of this work is the proposal of a fusion scenario combining image metrics and traditional HD-based approaches. In contrast to common believe that original iris textures exhibit too much variation to be used directly for recognition we proof that (1) quality metrics, interpreting iris textures as a noisy reproduction of the reference sample, can be employed for recognition, and (2) global features extracted by image metrics tend to complement localized features encoded by traditional feature extraction methods.

This paper is organized as follows: related work is reviewed in Section II. Subsequently, the proposed fusion scenario is described in detail in Section III. Experimental results are presented in Section IV. Section V concludes the paper.

II. Related Work

In the context of iris biometrics, image quality metrics are largely understood as domain-specific indicators to be considered for quality checks rejecting samples if insufficiently suited for comparison [4]. Such metrics have also been applied for dynamic matcher selection in biometric fusion scenarios [5], i.e. quality is employed to predict matching performance and to select the comparator or adjust weighting of the fusion rule. In contrast, in the proposed work general purpose image quality metrics and their ability to measure the degree of similarity between an original (enrollment sample) and degraded version of an image (sample) are employed. In the proposed model, the degradation of a sample to be compared does not result from compression, but by biometric noise factors (time, illumination, etc.), and the stored biometric gallery template represents the (updated) ideal representation of the biometric property of an individual.

Information fusion in biometrics is an efficient means to enhance the accuracy of a biometric system by employing multiple modalities, sensors, or comparators [6]. Compared to other types of fusion, score level fusion enables transparent enhancement of biometric systems by combining the matching scores of multiple comparators yielding a score vector $S = (s_1, \ldots, s_m)$, which is combined using a fusion rule, e.g. sum rule $s = \sum_{i=1}^{m} s_i$ or product rule $s = \prod_{i=1}^{m} s_i$ [7]. Park *et al.*[8] investigate this fusion type for local and global Gabor feature-vector based algorithms and found their proposed SVM-based fusion of HD scores to outperform each single Gabor filter when restricting the features to reliable regions. In previous

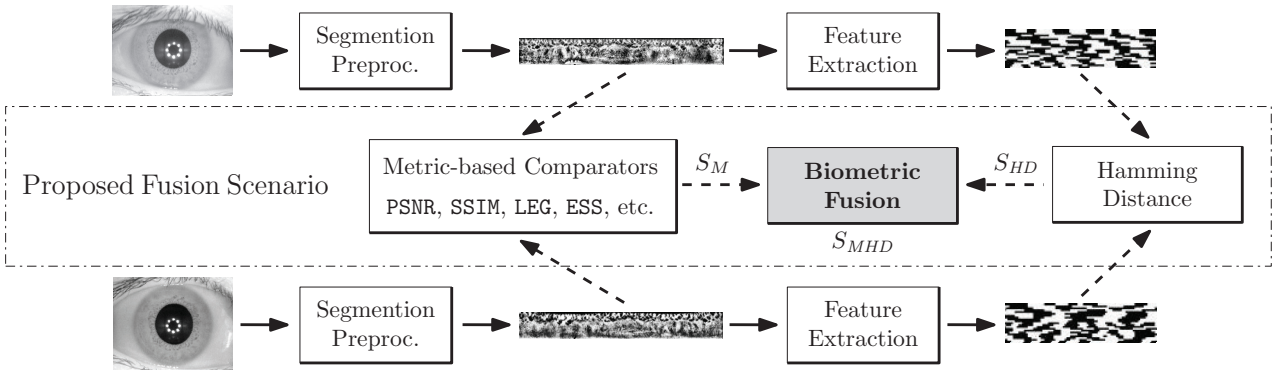

Fig. 1. Proposed Fusion Scenario: image quality metric-based scores are combined with Hamming distance-based feature-level scores to obtain a final score.

work [9], we have investigated score level fusion for combining best with worst HD-based alignment of iris codes for enhanced iris matching. If comparators are weakly dependent and still contain rich discriminative information, the combined score can be expected to provide better discrimination between genuine and imposter comparisons. An essential step before employing such fusion rules is a normalization of scores [6], which has been conducted manually by normalizing the mean of impostor score distributions for image metric-based comparators to 0.5 in this work.

III. Fusion of Iris Recognition Algorithms and Image Quality Metrics

The proposed fusion scenario is shown in Fig. 1. At the time of authentication, segmentation and pre-processing is performed on a given pair of iris images. Subsequently, resulting iris textures are compared applying a distinct image metric. The image quality metric-based comparison score, S_M, is normalized and fused with the according HD-based score, S_{HD}, after feature extraction has been applied to both iris textures, in order to obtain the final score S_{MHD}. The biometric fusion is performed by applying sum-rule fusion [6]:

$$S_{MHD} = \frac{1}{2}(S_M + S_{HD}). \quad (1)$$

In the following subsections modules of the proposed system, which comprise segmentation and pre-processing, iris-biometric feature extractors, and image metrics, are described in detail. All of the applied image metrics[1] are full reference metrics, meaning they utilize information from the original image O and impaired image I, both of size $W \times H$ to calculate an assessment of the visual similarity.

A. Pre-processing and Feature Extraction Algorithms

We apply multi-stage iris segmentation using a weighted version of adaptive Hough transform for iterative iris center detection at the first stage and pupillary and limbic boundary detection by applying an ellipsopolar transform and assessing gradient information for finding the second boundary based on the outcome of the first [10]. After having obtained a parametrization of inner and outer iris boundaries, the iris texture is unwrapped and normalized to a 512×64 pixel texture using Daugman's doubly dimensionless representation [2] and enhanced using contrast-limited adaptive histogram equalization [11]. Pre-processing is illustarted in Fig. 2.

In the feature extraction stage we employ custom implementations of two different algorithms used to extract binary iris-codes. The first one was proposed by Ma *et al.* [12]. Within this approach the texture is divided into 10 stripes to obtain 5 one-dimensional signals, each one averaged from the pixels of 5 adjacent rows, hence, the upper 512×50 pixel of preprocessed iris textures are analyzed. A dyadic wavelet transform is then performed on each of the resulting 10 signals, and two fixed subbands are selected from each transform. In each subband all local minima and maxima above an adequate threshold are located, and a bit-code alternating between 0 and 1 at each extreme point is extracted. Using 512 bits per signal, the final code is then 512×20 = 10240 bit. The second feature extraction method follows an implementation by Masek[2] applying filters obtained from a Log-Gabor function. Here, a row-wise convolution with a complex Log-Gabor filter is performed on the texture pixels. We use the same texture size and row-averaging into 10 signals prior to applying the one-dimensional Log-Gabor filter. The 2 bits of phase information are used to generate a binary code, which therefore is again 512×20 = 10240 bit.

B. Peak Signal to Noise Ratio (PSNR)

The PSNR is still widely used because it is unrivaled in speed and ease of use. However, it is also well known that the correlation to human judgment is somewhat lacking.

The following steps are performed to calculate the PSNR, where M is the maximum possible pixel value of the image.

[1]Implementation available at `www.wavelab.at/sources/VQI/`, except for VIF for which we used MetriX MuX from `foulard.ece.cornell.edu/gaubatz/metrix_mux`.

[2]L. Masek: Recognition of Human Iris Patterns for Biometric Identification, Master's thesis, University of Western Australia, 2003

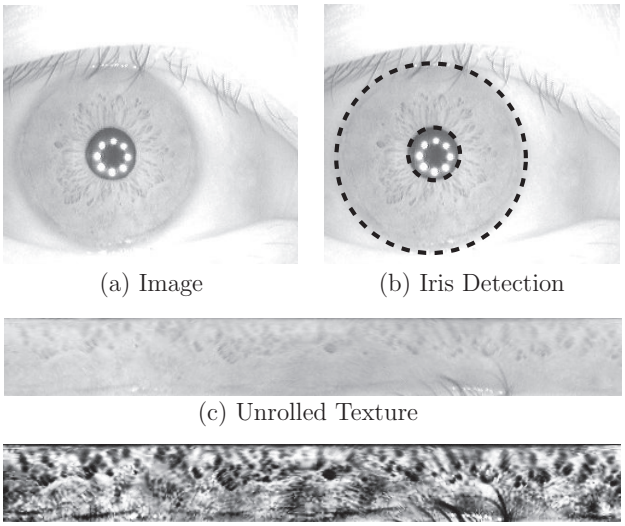

(a) Image (b) Iris Detection

(c) Unrolled Texture

(d) Enhanced Texture

Fig. 2. Preprocessing: (a) image of eye (b) detection of pupil and iris (c) unrolled iris texture (d) preprocessed iris texture.

Step 1: Calculate the mean squared error $\mathrm{MSE} = \frac{1}{WH} * \sum_{i=1}^{W}\sum_{j=i}^{H}(I(i,j)-O(i,j))^2$

Step 2: The PSNR is calculated:

$$\mathrm{PSNR} = 10\log_{10}\Big(\frac{M^2}{\mathrm{MSE}}\Big). \tag{2}$$

C. Structural Similarity Index Measure (SSIM)

The SSIM by Wang *et al.*[13] uses the local luminance as well as global contrast and a structural feature.

Step 1: Each image is transformed by convolution with a 11×11 Gaussian filter.

Step 2: The luminance, contrast and structural scores can be calculated and combined in one step as follows.

$$\mathrm{SSIM}(I,O) = \frac{(2\mu_I\mu_O + c_1)(2\sigma_{IO} + c_2)}{(\mu_I^2 + \mu_O^2 + c_1)(\sigma_I^2 + \sigma_O^2 + c_2)}, \tag{3}$$

where μ_I is the average pixel value of image I, σ_I^2 is the variance of pixel values of image I and σ_{IO} is the covariance of I and O. The variables $c_1 = (k_1 M)^2$ and $c_2 = (k_2 M)^2$, with $k_1 = 0.01$ and $k_2 = 0.03$, are used to stabilize the division.

D. Local Edge Gradients Metric (LEG)

The image metric based on local edge gradients was introduced by Hofbauer and Uhl [14] and uses luminance and localized edge information from different frequency domains.

Step 1: First the global luminance difference between I and O is calculated as $\mathrm{LUM}(I,O) = 1 - \sqrt{\frac{|\mu(O)-\mu(I)|}{M}}$, where $\mu(X) = \frac{1}{WH}\sum_{x=1}^{W}\sum_{y=1}^{H}X(x,y)$, and $X(x,y)$ is the pixel value of image X at position x, y.

Step 2: One step wavelet decomposition with Haar wavelets resulting in four sub images for each image X denoted as X_0 for the LL-subband, and X_1, X_2, X_3 for LH, HH and HL subbands, respectively.

Step 3: A local edge map is calculated for each position x, y in the image, reflecting the change in coarse structure. $\mathrm{LE}(I,O,x,y) = \max(0, \mathrm{EDC}(I,O,x,y) - 6)/2$, i.e. $\mathrm{LE} = 1$ if $\mathrm{EDC} = 8$, $\mathrm{LE} = 0.5$ if $\mathrm{EDC} = 7$ and 0 otherwise. In this case $\mathrm{EDC}(I,O,x,y) = \sum_{p\in N(x,y)}\mathrm{ED}(I,O,x,y,p)$, where $N(x,y)$ is the eight neighborhood of the pixel x, y, with $\mathrm{ED}(I,O,x,y,p) = 1$ if edge directions for I and O match, i.e. if $I(x,y) < I(p)$ and $O(x,y) < O(p)$ or $I(x,y) > I(p)$ and $O(x,y) > O(p)$, otherwise $\mathrm{ED}(I,O,x,y,p) = 0$.

Step 4: In order to assess the contrast changes a difference of gradients in a neighborhood is calculated by $\mathrm{LED}(I,O,x,y) = \frac{1}{8}\sum_{p\in N(x,y)}\left(1 - \sqrt{\frac{|LD(I,O,x,y,p)|}{M}}\right)^2$, with $\mathrm{LD}(I,O,x,y,p) = (O(x,y) - O(p)) - (I(x,y) - I(p))$.

Step 5: The edge score is calculated by combining local edge conformity (LE) and local edge difference (LED) into

$$\mathrm{ES}(I,O) = \frac{4}{WH}\sum_{x=1}^{\frac{W}{2}}\sum_{y=1}^{\frac{H}{2}}\Big(\mathrm{LE}(I_0,O_0,x,y) * \frac{1}{3}\sum_{i=1}^{3}\mathrm{LED}(I_i,O_i,x,y)\Big).$$

Step 6: The LEG visual quality index is calculated by combining ES and LUM.

$$\mathrm{LEG}(I,O) = \mathrm{LUM}(I,O)\,\mathrm{ES}(I,O). \tag{4}$$

E. Edge Similarity Score (ESS)

The ESS was introduced by Mao and Wu [15] and uses localized edge information to compare two images.

Step 1: Each image is separate into N blocks of size 8×8.

Step 2: For each image I a Sobel edge detection filter is used on each block i to find the most prominent edge direction $e_I^i$and quantized into one of eight directions (each corresponding to $22.5°$). Edge direction 0 is used if no edge was found in the block.

Step 3: Calculate the ESS based on the prominent edges of each block:

$$\mathrm{ESS} = \frac{\sum_{i=1}^{N} w(e_I^i, e_O^i)}{\sum_{i=1}^{N} c(e_I^i, e_O^i)}, \tag{5}$$

where $w(e_1, e_2)$ is a weighting function defined as

$$w(e_1,e_2) = \begin{cases} 0 & \text{if } e_1 = 0 \text{ or } e_2 = 0 \\ |cos(\phi(e_1) - \phi(e_2))| & \text{otherwise,} \end{cases}$$

where $\phi(e)$ is the representative edge angle for an index e, and $c(e_1, e_2)$ is an indicator function defined as $c(e_1, e_2) = 0$ if $e_1 = e_2 = 0$ and $c(e_1, e_2) = 1$ otherwise. In cases where $\sum_{i=1}^{N} c(e_I^i, e_O^i) = 0$ the ESS is set to 0.5.

F. Local Feature Based Visual Security (LFBVS)

The LFBVS was introduced by Tong et al. [16] utilizes localized edge and luminance features which are combined and weighted according to error magnitude, i.e. error pooling.

Step 1: Separate an image I into N blocks B_i^I of size 16×16.

Step 2: Calculate the average $\mu(B_i^I)$ and standard deviation $\sigma(B_i^I)$ of the pixel luminance values in the given block. Calculate the local luminance feature $\mathrm{LUM}(I,O,i) = (|\mu(B_i^O) - \mu(B_i^I)| + |\sigma(B_i^O) - \sigma(B_i^I)|) \,/\, 2L_{\max}$.

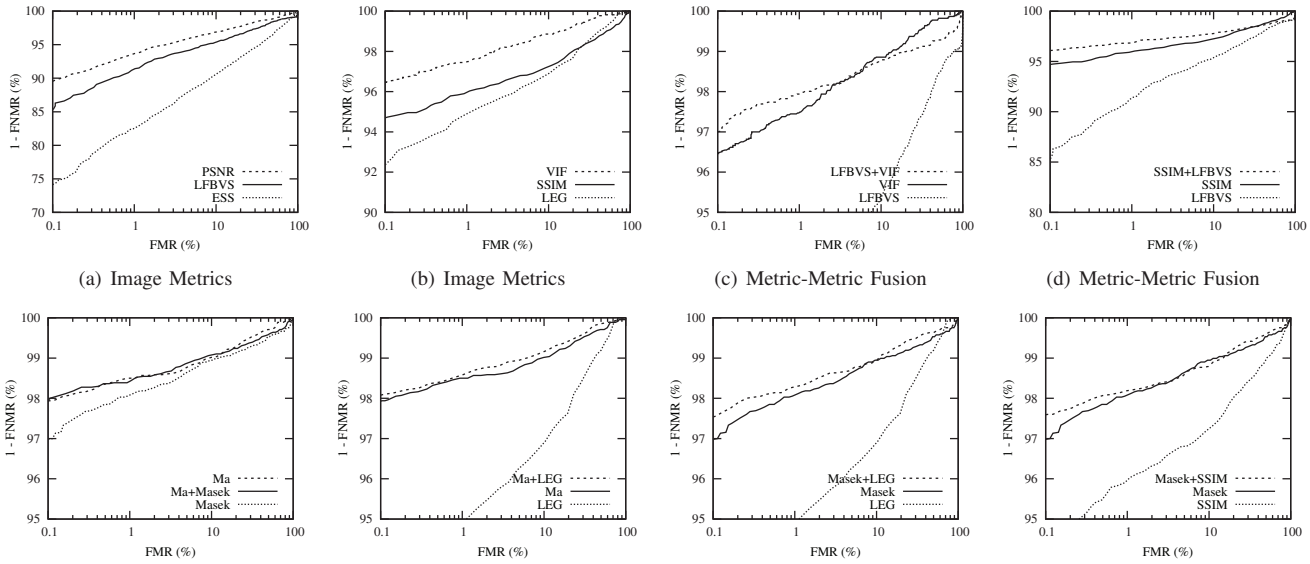

(a) Image Metrics (b) Image Metrics (c) Metric-Metric Fusion (d) Metric-Metric Fusion

(e) Trad. Algorithms (f) IrisCode-Metric Fusion (g) IrisCode-Metric Fusion (h) IrisCode-Metric Fusion

Fig. 3. Receiver Operation Characteristic (ROC) curves for image metric, traditional algorithms, and selected fusion scenarios of the proposed approach.

Step 3: For each pixel in the macroblock (excluding borders) calculate the (luminance) edge directions $\delta_x(x,y) = L(x+1,y) - L(x-1,y)$, $\delta_y(x,y) = L(x,y+1) - L(x,y-1)$. Generate a histogram $H_i^I[d] = A$ of cumulative edge amplitude strength $a = \sqrt{\delta_x(x,y)^2 + \delta_y(x,y)^2}$ over edge directions d(8-bins for 360^o) for each block. And using the histogram calculate local edge density feature $\mathrm{ED}(I,O,i) = \sum_{d=1}^{8} |H_i^O[d] - H_i^I[d]| \,/\, \sum_{d=1}^{8} \max(H_i^O[d], H_i^I[d])$

Step 4: Calculate a local visual score, i.e. local luminance and edge density $LVS(I,O,i) = 0.2LUM(I,O,i) + 0.8ED(I,O,i)$. Order local visual features $\mathrm{OLVS}(I,O,j) = \mathrm{LVS}(I,O,i_j)$ such that $\forall x < i_j \,\mathrm{LVS}(I,O,x) \leq \mathrm{LVS}(I,O,i_j)$ and $\forall x > i_j \,\mathrm{LVS}(I,O,x) \geq \mathrm{LVS}(I,O,i_j)$.

Step 5: Weigh the ordered local visual feature scores to further increase the prominent errors,

$$\mathrm{LFBVS}(I,O) = \sum_{i=1}^{N} \exp^{\frac{i}{N-0.5}} \mathrm{OLVS}(O,I,i) \,/\, \sum_{i=1}^{N} \exp^{\frac{i}{N-0.5}} . \quad (6)$$

G. Visual Information Fidelity (VIF)

The VIF by Sheikh and Bovik [17] uses a refined model which starts with the modeling of the reference image using natural scene statistics (NSS). Furthermore, the possible distortion is modeled as signal gain and additive noise in the wavelet domain and parts of the HVS which have not been covered by the NSS are modeled, i.e. internal neural noise is modeled by using a additive white Gaussian noise model. While the VIF can not be described in the available space the calculation roughly consists of the following steps.

Step 1: NSSs are calculated based on Gaussian scale mixture (GSM) model based on the wavelet domain.

Step 2: Calculate a model for the distorted image based on the GSM model from the original image combined with signal gain and additive noise in the wavelet domain (this compensates for white noise and image blur in the image domain).

Step 3: Extend the model to include information from HVS, i.e. optical point spread, contrast sensitivity and internal neural noise, which is not covered by the NSS model.

Step 4: Calculate the amount of the original signal, taking into account different wavelet subbands, which can be reconstructed from the distorted signal given the NSS and the HVS model, this reconstructible fraction of the original signal is termed VIF.

IV. Experimental Study

Experiments are carried out on the CASIA-v3-Interval iris database[3] using left-eye images only. The database consists of good quality 320×280 pixel NIR illuminated indoor images where the applied test set consists of 1307 instances, a sample is shown in Fig. 2 (a).

Recognition accuracy is evaluated in terms of false none match rate (FNMR) and false match rate (FMR). The FNMR defines the proportion of verification transactions with truthful claims of identity that are incorrectly rejected, and the FMR defines the proportion of verification transactions with wrongful claims of identity that are incorrectly confirmed (ISO/IEC FDIS 19795-1). As score distributions overlap the EER of the system is defined (FNMR = FMR). At all authentication attempts 7 circular texture-shifts and according bit-shift are performed in each direction for all comparators. Image metric scores are normalized in a way that mean impostor scores are 0.5 and low scores indicate high similarity. Obtained

[3]The Center of Biometrics and Security Research, CASIA Iris Image Database, `http://www.idealtest.org`

TABLE I
OBTAINED RESULTS FOR THE PROPOSED FUSION SCENARIO.

	EER (%)							
	Ma *et al.*	Masek	PSNR	SSIM	LEG	ESS	LFBVS	VIF
Ma *et al.*	1.43	1.46	1.56	1.53	**1.32**	2.51	2.01	1.65
Masek		1.77	1.97	**1.72**	**1.58**	2.43	2.12	1.78
PSNR			4.21	**3.08**	**3.34**	4.69	**3.60**	2.11
SSIM				3.40	3.40	4.51	**2.71**	2.18
LEG					3.99	5.76	**3.46**	2.10
ESS						9.61	**4.90**	2.20
LFBVS							5.54	**1.86**
VIF								2.06

performance rates in terms of EERs for single and paired combination of comparators are summarized in Table I. According ROC curves of individual image metrics and selected fusion scenarios, described feature extraction algorithms as well as selected fusion scenarios of image metrics and these are plotted in Fig. 3. It is important to note, that all combinations (IrisCode-Metric and Metric-Metric) represent a challenging single-sensor multi-algorithm fusion scenario.

A. Combination of Image Metrics

Focusing on obtained EERs most individual image metrics do not represent an alternative to traditional iris-based feature extraction algorithms, see Table I. While an exclusive application of best image metrics yield EERs $> 2\%$ (see Fig. 3 (a)-(b)), traditional feature extraction algorithms obtain EERs $< 1.5\%$ (see Fig. 3 (e)). However, as shown in Fig. 3 (c)-(d) distinct combinations of image metrics yield significant improvement in accuracy, e.g. a fusion of LFBVS and VIF yields an EER of 1.86%.

B. Combination of Metrics and Traditional Algorithms

For the applied simple sum-rule, a combination of applied feature extraction algorithms does not yield improvement with respect to recognition performance, see Fig. 3 (e). In addition, image metrics do not supplement traditional iris recognition algorithms in general. While the incorporation of most image metrics (e.g. PSNR, ESS and LFBVS) decreases performance distinct image metrics represent adequate complements (e.g. SSIM and LEG), see Table I and Fig. 3 (f)-(h). In particular, combinations of the LEG metric and applied feature extractors show significant improvements achieving EERs of 1.32% and 1.58%, respectively. Obtained results appear promising since image metrics are applied without any adaption using the most simple fusion rule to the proposed application scenario, i.e. adjusted implementations of image metrics are expected to further improve recognition accuracy.

V. CONCLUSION AND FUTURE WORK

In this paper a fusion of image metrics and traditional HD-based comparators is presented. It is demonstrated that the incorporation of distinct image metrics in a fusion scenario is able to significantly improve recognition accuracy of iris biometric systems.

Future work will comprise biometric fusions of several image metrics and traditional biometric comparators as well as an adaption of image metrics to biometric systems, e.g. by applying image metrics only to distinct parts of biometric data. Regarding security issues, image metrics will be assessed for comparing iris images in encrypted domain.

ACKNOWLEDGEMENTS

This work has been supported by the Austrian Science Fund, project no. L554-N15 and the Austrian FIT-IT Trust in IT-Systems, project no. 819382.

REFERENCES

[1] K. W. Bowyer, K. Hollingsworth, and P. J. Flynn, "Image understanding for iris biometrics: A survey," *Comp. Vis. Image Underst.*, vol. 110, no. 2, pp. 281 – 307, 2008.

[2] J. Daugman, "How iris recognition works," *IEEE Trans. Circ. and Syst. for Video Techn.*, vol. 14, no. 1, pp. 21–30, 2004.

[3] J. Daugman and C. Downing, "Effect of severe image compression on iris recognition performance," *IEEE Trans. Inf. Forensics and Sec.*, vol. 3, pp. 52–61, 2008.

[4] I. Tomeo-Reyes, J. Liu-Jimenez, I. Rubio-Polo, and B. Fernandez-Saavedra, "Quality metrics influence on iris recognition systems performance," in *IEEE Int'l Carnahan Conf. Sec. Techn. (ICCST)*, 2011, pp. 1–7.

[5] M. Vatsa, R. Singh, A. Noore, and A. Ross, "On the dynamic selection of biometric fusion algorithms," *IEEE Trans. Inf. Forensics and Sec.*, vol. 10, no. 3, pp. 470 – 479, 2010.

[6] A. Ross and A. K. Jain, "Information fusion in biometrics," *Pattern Recogn. Lett.*, vol. 24, no. 13, pp. 2115–2125, 2003.

[7] A. Uhl and P. Wild, "Single-sensor multi-instance fingerprint and eigenfinger recognition using (weighted) score combination methods," *Int'l J. on Biometrics*, vol. 1, no. 4, pp. 442–462, 2009.

[8] H.-A. Park and K. Park, "Iris recognition based on score level fusion by using svm," *Pattern Recogn. Lett.*, vol. 28, pp. 2019–2028, 2007.

[9] C. Rathgeb, A. Uhl, and P. Wild, "Shifting score fusion: On exploiting shifting variation in iris recognition," in *Proc. 26th ACM Symp. Appl. Comp. (SAC'11)*, 2011, pp. 1–5.

[10] A. Uhl and P. Wild, "Weighted adaptive hough and ellipsopolar transforms for real-time iris segmentation," in *Proc. Int'l Conf. on Biometrics (ICB)*, 2012, to appear.

[11] A. M. Reza, "Realization of the contrast limited adaptive histogram equalization (clahe) for real-time image enhancement," *J. VLSI Signal Process. Syst.*, vol. 38, no. 1, pp. 35–44, 2004.

[12] L. Ma, T. Tan, Y. Wang, and D. Zhang, "Efficient iris recognition by characterizing key local variations," *IEEE Trans. Image Proc.*, vol. 13, no. 6, pp. 739–750, 2004.

[13] Z. Wang, A. Bovik, H. Sheikh, and E. Simoncelli, "Image quality assessment: from error visibility to structural similarity," *IEEE Trans. Image Proc.*, vol. 13, no. 4, pp. 600–612, 2004.

[14] H. Hofbauer and A. Uhl, "An effective and efficient visual quality index based on local edge gradients," in *IEEE 3rd Europ. Workshop on Visual Inf. Proc.*, 2011, p. 6pp.

[15] Y. Mao and M. Wu, "Security evaluation for communication-friendly encryption of multimedia," in *IEEE Int'l Conf. on Image Proc. (ICIP)*, 2004.

[16] L. Tong, F. Dai, Y. Zhang, and J. Li, "Visual security evaluation for video encryption," in *Proc. Int'l Conf. on Multimedia*, ser. MM '10, 2010, pp. 835–838.

[17] H. R. Sheikh and A. C. Bovik, "Image information and visual quality," *IEEE Trans. on Image Proc.*, vol. 15, no. 2, pp. 430–444, May 2006.